Initial adsorption of Co on Cu(001): A first-principles investigation

Rossitza Pentcheva and Matthias Scheffler
Fritz-Haber-Institut der Max-Planck-Gesellschaft, Faradayweg 4-6, D-14195 Berlin-Dahlem, Germany
(Received 4 January 2002; published 3 April 2002)

We present total-energy calculations for the initial adsorption of Co on Cu(001). By studying different adsorption geometries we find that the substitutional adsorption is strongly favored compared to the on-surface adsorption at a fourfold hollow site. The electronic and structural effects actuating this tendency are analyzed. We investigated the coverage dependence of the adsorption energy and find that it is particularly favorable for low coverages ($\theta<0.25$ ML) while at higher coverages we predict the formation of compact islands. In addition the paper also explores the influence of magnetism. We find that magnetic Co adatoms induce a weak spin polarization in the substrate with an oscillatory character: nearest Cu adatoms couple parallel while next-nearest adatoms couple antiparallel. However, we find that spin polarization has little influence on the energetic trends. Due to the tendency of deposited Co to adsorb substitutionally, it follows that under initial growth conditions two different mobile adatom sorts will be on the surface, on-surface Co (not yet incorporated substitutionally) as well as Cu created by the already substitutionally incorporated Co. The role of the substitutional Co atoms as pinning centers for subsequent island nucleation is investigated quantitatively.

DOI: 10.1103/PhysRevB.65.155418 PACS number(s): 68.55.−a, 68.35.−p, 71.20.Be, 75.70.Rf

I. INTRODUCTION

Experimental techniques like atomic force and scanning tunneling microscopy and theoretical approaches based on the density-functional theory (DFT) represent a powerful tool to study the early stages of growth on an atomic scale. The current understanding of epitaxial growth is that deposited atoms diffuse between high-symmetry on-surface sites and typically island nuclei are formed due to binary collisions where often a dimer represents a stable island.[1] However, it is questionable whether this picture applies also in the case of heteroepitaxy and, indeed, it was shown that in this case other scenarios may become relevant:[2,3] e.g., it is possible that the diffusing adatom exchanges sites with a substrate atom and is incorporated in the substrate layer, and thus already the monomer constitutes a stable nucleus. Substitutional adsorption and possibly even the formation of a surface alloy can occur even for materials that are immiscible in the bulk as recently reported, for example, for Na on Al(100) and Al(111),[4,5] Mn on Cu(001),[6] Fe on Cu(001),[7] and Cr on Fe(001).[8,9]

Co on Cu(001) is another system where intermixing was observed.[10] As shown in a recent combined scanning tunneling microscoy (STM) and *ab initio* study[11] the thermally activated exchange processes have surprising consequences on the growth of Co on Cu(001). A *bimodal* growth mode with respect to island sizes and chemical composition was predicted theoretically and evidenced in a CO-titration experiment and in the island-size distribution from STM. The main features of this growth mode are large copper islands with Co decoration at the edges and a high density of small Co islands. The role of substitutional Co atoms as centers for island nucleation and the high mobility of the kicked-out copper atoms were identified as the microscopic mechanisms that initiate the *bimodal* growth.

In this paper we establish a connection between the energetic trends reported in Ref. 11 and the underlying electronic and magnetic effects. Furthermore, we extend our study to the coverage dependence of the adsorption energy and the change of work function upon adsorption. The paper is organized as follows. Details on the calculations are given in Sec. II. Two different adsorption geometries are studied for submonolayer cobalt coverages in Sec. III: on-surface adsorption, where the adatom occupies a fourfold hollow sites on the surface, and substitutional, where it exchanges sites with a substrate atom and is incorporated in the substrate layer. The energetic trends are explained in the light of the structural and electronic effects that take place upon adsorption. In Sec. IV we investigate different coverages ($0<\Theta\leqslant 1$ ML) to identify the importance of the adatom-adatom versus adatom-substrate interaction. We further consider the stability of monolayer-thick surface alloys against phase separation in compact Co islands and its dependence on coverage. The influence of magnetism on the energetic trends and the magnetic properties of the adsorbate systems are discussed in Sec. V. Finally, in Sec. VI we investigate the role of the substituted cobalt atoms as nucleation centers for diffusing Co and Cu adatoms on the surface and the consequences for the surface morphology. Parallels and differences to other heteroepitaxial systems like alkali on Al(100) and Al(111) (Refs. 4 and 5) and $3d$ transition-metal adatoms on Fe(001) (Ref. 9) are discussed. The results are summarized in Sec. VII.

II. CALCULATIONAL DETAILS

Our calculations are performed using density-functional theory with the exchange-correlation functional treated in the local-density approximation (LDA).[12] For the magnetic systems we performed spin-polarized calculations in the local spin-density approximation (LSDA). We also examined the possible importance of nonlocal exchange and correlation effects by employing the generalized-gradient approximation (GGA) in the parametrization of Perdew, Burke, and Ernzerhof.[13] The results show that for our study the LDA and GGA give the same energetic trends. More details on this issue will be discussed in the Appendix.

The eigenvalue problem was solved applying the full-potential linearized augmented-plane-wave (FP-LAPW) method as implemented in the WIEN97 code.[14,15] The surface is simulated by repeated slabs separated in the z direction by a vacuum region. Co is adsorbed on both sides of the substrate. Geometries are optimized by damped Newton dynamics[16] and the relaxations are given with respect to the interlayer spacing of a Cu crystal.

The lateral lattice parameter of the Cu substrate was set to the value calculated for a fcc copper crystal (nonrelativistic calculation), $a_{\mathrm{Cu}}=3.55$ Å. We note that the calculated lattice constant of the substrate is 1.6% smaller than the measured one (3.61 Å), 0.1% of which reflects our neglect of zero-point vibrations in the theory. We chose a muffin tin (MT) radius of $R_{\mathrm{Cu}}^{\mathrm{MT}}=2.20$ bohrs for the Cu atoms and a slightly smaller radius $R_{\mathrm{Co}}^{\mathrm{MT}}=2.15$ bohrs for the Co atoms to prevent overlap of the MT spheres upon the strong relaxation found for some systems.

The Cu(001) surface was modeled by a five-layer copper slab which ensures that the interaction of the adsorbates through the substrate is negligible for the questions of interest in this paper. The thickness of the vacuum between the repeated slabs amounts to 18 Å. The cutoff parameters used in the LAPW calculation are summarized shortly in the following, for more details the reader is referred to a previous work:[32] in the muffin tin spheres the wave functions were expanded in spherical harmonics with an angular momentum up to $l_{\mathrm{max}}^{\mathrm{wf}}=10$. Nonspherical contributions to the electron density and potential within the MTs were considered up to $l_{\mathrm{max}}^{\mathrm{pot}}=4$. The cutoff for the Fourier-series expansion of the interstitial electron density and potential was chosen to be $G_{\mathrm{max}}=12.0$ bohr^{-1} and the cutoff for the plane wave basis set $E_{\mathrm{cut}}=15.6$ Ry. The Brillouin-zone integration was performed with a special $\mathbf{k}_{\parallel}$-point set generated after the scheme of Monkhorst and Pack.[17] An accuracy better than 1% is obtained by using 144 $\mathbf{k}_{\parallel}$ points in the Brillouin zone (BZ) for a $p(1\times1)$ structure. For the bigger unit cells, $c(2\times2)$, $p(2\times2)$, and $p(3\times3)$, we use a corresponding mesh of 100, 36, and 16 $\mathbf{k}_{\parallel}$ points in the BZ, respectively, so as to obtain the same sampling in reciprocal space. For energy differences the numerical accuracy is better than 0.02 eV per atom.

The bulk and free atom energies needed as a reference to determine the adsorption energy [see Eq. (1)] were calculated for the same LAPW parameters as in the slab calculations. For the bulk calculation 104 $\mathbf{k}$ points in the irreducible wedge of the BZ were used. The isolated atom was simulated in a box with next-nearest-neighbor distance of 15 bohrs to avoid an interaction between atoms in the neighboring unit cells. The cohesive energies for fcc Cu and Co within LDA (4.50 eV and 6.48 eV, respectively) are in good agreement with previous calculations[18] and by 1.0 eV and 2.09 eV higher than the experimental values cited therein. We note that the overestimation of the cohesive energy compared to experiment is a well-known effect of LDA.

III. ON-SURFACE VERSUS SUBSTITUTIONAL SITE: STRUCTURAL, ENERGETIC, AND ELECTRONIC TRENDS

Experimental results[10,11] suggest that after deposition of submonolayer coverages of Co on Cu(001) the surface is intermixed. However, due to the interplay of electronic and geometric effects, the chemical nature of atoms and the composition of islands can typically not be identified unambiguously if only STM-topography data are available. Therefore we performed total-energy calculations for two different adsorption geometries—on-surface with a Co atom on a fcc hollow site and substitutional with the Co atom incorporated in the substrate layer—and found that the substitutional adsorption is strongly favored.[11] In this section we discuss the energetic stability and the electronic and structural effects accompanying the adsorption process.

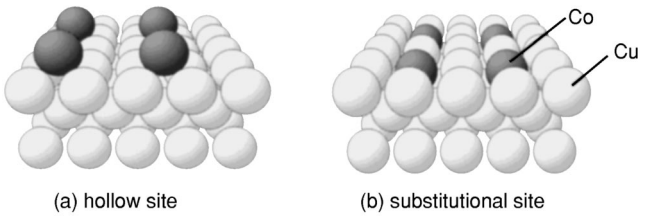

FIG. 1. Side view of a Cu(001)-$p(2\times2)$-Co structure with Co adatoms at (a) on-surface hollow and (b) substitutional adsorption sites.

The geometries of a $p(2\times2)$ structure with Co atoms on a fcc hollow or substitutional site, marked as Cu(001)-$p(2\times2)$-Co and Cu(001)-$p(2\times2)$-Co-sub, respectively, are shown in Fig. 1. For the on-surface adsorption in a $p(2\times2)$ geometry we found a substantial reduction (16%) of the distance between adsorbate and substrate layer with respect to the interlayer spacing of the copper crystal, causing an energy gain of 0.28 eV compared to the unrelaxed structure. This relaxation is connected with a decrease of the next-nearest Co-Cu neighbor distance by 8% compared to the interatomic distance in fcc Cu bulk. On the other hand for Cu(001)-$p(2\times2)$-Co-sub the adatom relaxes -7% (inwards), while the Cu atoms in the surface layer relax by -3%. Thus the relative relaxation of the Co adatom with respect to the Cu surface layer is -4%. The energy gain due to relaxation is negligible in this case.

Epitaxial growth is a nonequilibrium situation. However, if the deposition rate is not too high, structures in local thermal equilibrium can evolve. For this reason we determine stable and metastable geometries with respect to the adsorption energy per cobalt adatom; e.g., if 0.25 ML of cobalt are adsorbed on the surface the adsorption energy E^{ad} is defined as

$$E^{\mathrm{ad}}=\frac{1}{2}(E^{\mathrm{Cu(001)}}-2N^{\mathrm{Cu}}E^{\mathrm{Cu\text{-}bulk}}+2N^{\mathrm{Co}}E^{\mathrm{Co\text{-}atom}}-E^{\mathrm{Cu(001)\text{-}(2\times2)\text{-}Co}}). \quad (1)$$

Here $E^{\mathrm{Cu(001)}}$ and $E^{\mathrm{Cu(001)\text{-}(2\times2)\text{-}Co}}$ are the total energies of a clean copper surface and the adsorbate system, respectively, $E^{\mathrm{Cu\text{-}bulk}}$ is the fcc bulk energy of Cu, and $E^{\mathrm{Co\text{-}atom}}$ is the energy of the free-spin-polarized Co atom. The factor of $\frac{1}{2}$ in Eq. (1) accounts for the presence of two surfaces of the slab. The adsorption energy for the on-surface adsorption ($N^{\mathrm{Cu}}=0$, $N^{\mathrm{Co}}=1$) is $E_{\mathrm{on\text{-}surf}}^{\mathrm{ad}}=3.94$ eV. For substitutional adsorption, where the cobalt atom exchanges a copper atom in

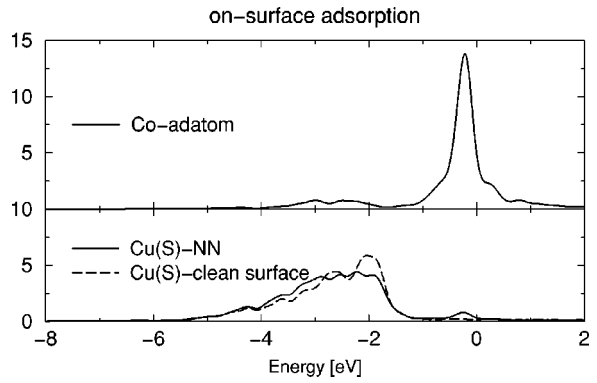

FIG. 2. The muffin tin contributions to the total density of states of the Co adatom and its Cu nearest-neighbor [Cu(S)-NN] in Cu(001)-$p(2\times2)$-Co (solid line) and of the corresponding Cu atom in the clean Cu(001) surface (dashed line). The calculated DOS were broadened by a Gaussian with a width of $2\sigma=0.2$ eV.

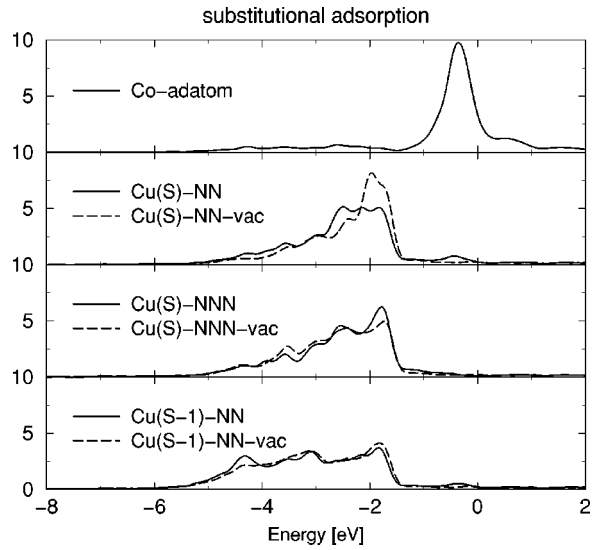

FIG. 3. The muffin tin contributions to the total density of states of the Co adatom and the neighboring Cu atoms in Cu(001)-$p(2\times2)$-Co-sub (solid line) and of the corresponding Cu atoms in a $p(2\times2)$ vacancy structure (dashed line). The nearest and next-nearest neighbors of the Co atom in the surface layer are labeled as Cu(S)-NN and Cu(S)-NNN, respectively, while the nearest neighbor from the subsurface layer is Cu(S-1)-NN. The calculated DOS were broadened by a Gaussian with a width of $2\sigma=0.2$ eV.

the substrate layer, the expelled Cu adatom is assumed to diffuse to a step and be rebound at a kink site where its energy equals the cohesive energy of copper[19] ($N^{\mathrm{Cu}}=N^{\mathrm{Co}}=1$). In this case we obtain $E_{\mathrm{sub}}^{\mathrm{ad}}=5.26$ eV; i.e., the substitutional adsorption is energetically favored by 1.32 eV over the on-surface adsorption.

The substitutional adsorption, as defined in Eq. (1), can be considered as a composite process, consisting of the removal of a surface Cu atom, the adsorption of the Co adatom into the so-formed surface vacancy, and the subsequent adsorption of the Cu atom at a kink site of a copper step or island. This scenario is very likely because the copper adatoms are quite mobile[20] and therefore should be able to reach steps which exist on the surface under normal growth conditions. We also considered an intermediate state of the composite process where the kicked out Cu adatom occupies a fourfold hollow site as a nearest neighbor of the embedded Co atom [see Fig. 10(a)]. For 0.11 ML of Co in a $p(3\times3)$ geometry the energy difference between the on-surface Co and intermediate-state configuration amounts to 0.72 eV, compared to 1.36 eV for the final state of the exchange process, as defined in Eq. (1). Thus, the remaining 0.64 eV is the energy gain of the copper adatom at a kink site compared to Cu as a nearest neighbor of the embedded Co atom. In a recent second-moment tight-binding approximation (TB-SMA) study, where the *N*-body potentials were fitted to experimental elastic constants and first-principles values, Levanov *et al.*[21] found the energy gain between the initial (on-surface) and intermediate state (which they called ''direct'' exchange) to be 0.50 eV, which gives the same qualitative trend as the DFT-LDA result.

In order to understand this result one has to keep in mind that the *d* states of cobalt take part in the chemical bonding. Thus, cobalt prefers to occupy a highly coordinated site. In the on-surface adsorption geometry the cobalt adatom has four Cu neighbors, whereas in the substitutional adsorption the Co atom has eight nearest neighbors. The electronic effects connected with the adsorption of cobalt are displayed in Figs. 2 and 3. The solid lines represent the muffin tin contributions to the total density of states (DOS) of the Co adatom and its nearest (NN) and next-nearest (NNN) Cu neighbors in the surface and subsurface layer for both adsorption geometries. The position of the Fermi level relative to the peaks in the density of states determines the occupation of the states and the nature of bonding. For a free-standing Co-$p(2\times2)$ layer (not shown here) the Fermi level crosses the narrow atomiclike $3d$ band close to the peak maximum. In the adsorbate systems the interaction with the substrate leads to a broadening of the Co *d* band and a relative shift towards lower energies and a lower DOS at the Fermi level. This effect is particularly distinct for the substitutional site and can be directly related to the stronger bonding at the substitutional geometry.

The adsorption of cobalt on the surface invokes significant changes in the DOS of the substrate surface. The MT contributions of the substrate atoms to the total DOS before and after adsorption are plotted in Figs. 2 and 3 with a solid and dashed line, respectively. In the case of on-surface adsorption (Fig. 2) the DOS of copper in the substrate surface layer is reduced at the top of the *d* band and the *d* band is slightly broadened. Additionally we observe an enhancement at the position of the Co *d* band near the Fermi level which indicates the hybridization of the substrate *sp* bands with the adsorbate *d* band. For the substitutional adsorption, Fig. 3, the strongest changes occur for the nearest neighbor in the surface layer [Cu(S)-NN]: filling the vacancy with a Co adatom leads to a broadening of the Cu *d* band and a substantial reduction of the DOS at the top of the *d* band, resulting in a shift of the *d*-band center of mass towards lower energies. The adsorption-induced changes in the next-nearest neighbors in the surface layer [Cu(S)-NNN] and the nearest

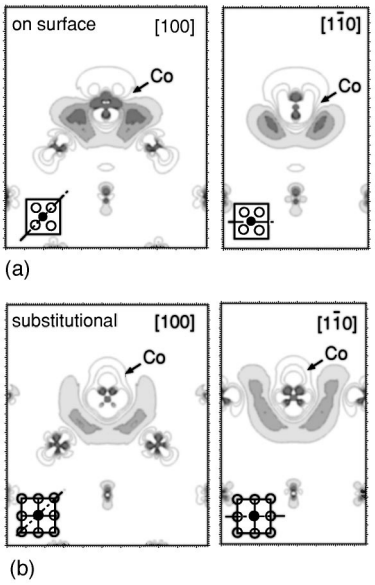

FIG. 4. Electron density difference $n(\mathbf{r})-n^{\mathrm{ref}}(\mathbf{r})-n^{\mathrm{Co}\text{-}p(2\times2)}(\mathbf{r})$ of a $p(2\times2)$ structure with Co adatom at on-surface (upper panel) or substitutional (lower panel) adsorption sites. $n(\mathbf{r})$, $n^{\mathrm{ref}}(\mathbf{r})$, and $n^{\mathrm{Co}\text{-}p(2\times2)}(\mathbf{r})$ are the electron densities of the adsorbate system, the reference system [clean Cu(001) or vacancy structure], and a free Co-(2×2) monolayer. The grey regions correspond to regions of electron-density increase while regions of electron-density depletion are marked only by contour lines. The contour lines start at $\pm2\times10^{-3}$ bohr^{-3} and have a separation of 4×10^{-3} bohr^{-3}. The plots show a cross section along the (100) and $(1\bar{1}0)$ planes. The top view of the surface unit cell with the direction of the cut is given schematically in the left corner of each picture.

neighbors in the subsurface layer [Cu(S-1)-NN] are significantly smaller and for Cu(S)-NNN have even the opposite character.

Additional insight into the bonding nature can be gained from Fig. 4 showing the change in the electron density upon adsorption. For the on-surface adsorption $\Delta n(\mathbf{r})$ is given with respect to the clean Cu(001) surface and a free-standing Co-$p(2\times2)$ monolayer and for the substitutional adsorption with respect to a vacancy structure and a free-standing $p(2\times2)$-Co monolayer with Co and Cu atoms at the corresponding positions as in the Co adsorbate system. The electron-density plots show that the perturbation caused by the adsorption does not reach very far into the substrate and is essentially restricted to the neighboring Cu atoms. In both cases charge is transferred from the vacuum side of the adsorbate towards the interstitial region with a pronounced accumulation of electron charge between the Co adatom and its Cu neighbors. For the on-surface adsorption the bonds are formed between the adsorbate and the Cu atoms of the top Cu layer while for the substitutional adsorption the bonds are formed both with the Cu atoms of the top Cu layer and the Cu neighbors from the subsurface layer. Due to the electron charge accumulation on the line between the adatom and Cu neighbors, the bonding mechanism shows a directional covalent character.

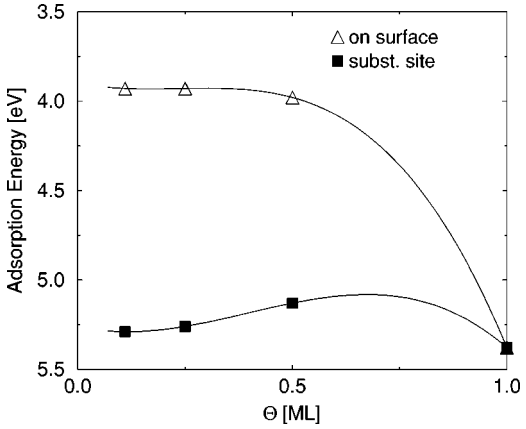

FIG. 5. The adsorption energy E^{ad} in eV per Co atom as a function of coverage for a Co adatom on a fcc hollow (triangles up) and a substitutional (solid squares) site. In the limit of $\Theta=1.0$ ML the adsorption energy of a Co adlayer on Cu(001) represents an estimate of E^{ad} of a large compact Co island.

IV. DEPENDENCE OF E^{ad} ON COVERAGE

The above discussion dealt with the adsorption of 0.25 monolayers of Co on Cu(001). We also studied the interplay of the adatom-adatom versus adatom-substrate interaction for different Co coverages. In Fig. 5 the adsorption energy E^{ad} is plotted as a function of the adsorbate coverage. For all coverages the adsorption energy for the substitutional site is higher than the one for the fcc hollow site and thus the former is always more favorable than the latter.

A further aspect that needs to be considered is whether the surface alloys formed through substitutional adsorption are stable against separation into compact islands. In the limit of 1 ML the two adsorbate configurations coincide. The adsorption energy of a sufficiently large compact island, where the contribution of the side walls is small, can be expressed by the one of the $p(1\times1)$ cobalt monolayer on Cu(001), which equals 5.38 eV. Figure 5 shows that the substitutional adsorption always competes with the formation of compact islands. However, for $\Theta\leqslant0.25$ ML the probability that Co adatoms meet and form islands is low. In this case, single cobalt adatoms prefer to adsorb substitutionally and achieve a higher coordination of Cu atoms (8 compared to 4 for the on-surface adsorption). However, Co-Co bonds are stronger than Co-Cu bonds. Therefore at higher coverages which correspond to shorter adsorbate-adsorbate distances the interaction between the localized *d* orbitals becomes important and a close-packed Co structure will be attained. In agreement with previous theoretical studies[22] a $c(2\times2)$-surface alloy of cobalt on Cu(001) is unstable against phase separation. Fassbender *et al.*[10] and Chambliss and Johnson[7] proposed recently that the surface intermixing of Co or Fe on Cu(001) is a result of the difference of the surface free energies of the contributing materials. However, our calculations show that the difference of surface energies is rather the driving force towards the thermodynamic equilibrium configuration, a compact bilayer thick Co island capped by copper.[32] The substitutional adsorption represents an alternative only for low coverages when the Co adatoms whose mobility is re-

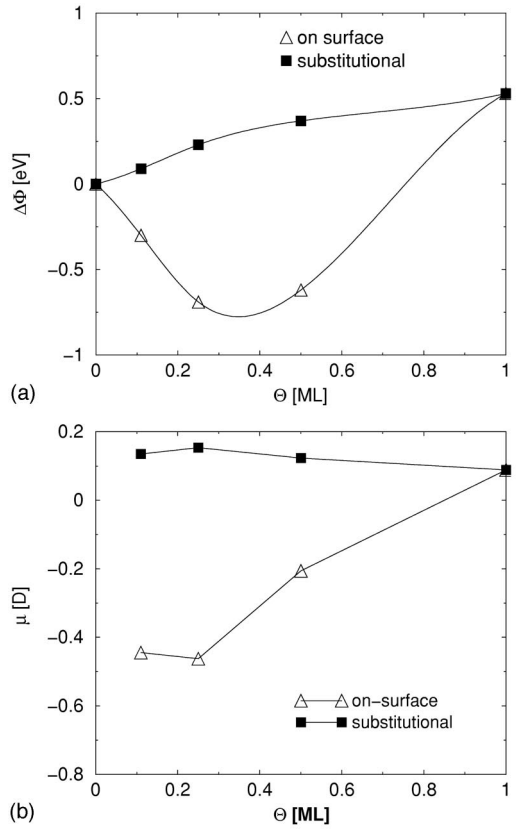

FIG. 6. The change of work function $\Delta\Phi$ in eV compared to the clean Cu(001) surface and the induced dipole moment μ in debye as a function of coverage for a Co adatom on a fcc hollow (triangles up) and a substitutional (filled squares) site. In the limit of $\Theta=1.0$ ML, $\Delta\Phi$ and μ correspond to the ones of a Co adlayer on Cu(001).

stricted by higher diffusion barriers[23,24] do not feel the presence of other Co atoms.

The adsorption of alkali-metal atoms (e.g., Na) on Al(001) and Al(111) (Refs. 4 and 5) was the first example of surface alloying of immiscible materials. However, concerning the coverage dependence, the situation for Na on Al(001) is the opposite compared to Co on Cu(001): Substitutional adsorption does not occur for single adatoms, but only after the coverage has reached a critical value. In this case intermixing is driven by the strong electrostatic repulsion between the adatoms where the adsorption at substitutional sites enables a better screening and thus reduces the electrostatic interaction. In the case of Co on Cu(001) the changes of the work function, $\Delta\Phi$, with respect to the work function of the bare surface $\Phi_{\mathrm{Cu}(001)}=4.78$ eV are much lower than for alkali metal adsorbates. Consequently, the induced dipole moments, which are given by the Helmholz equation, $\mu\propto\Delta\Phi/\Theta$, are small and the electrostatic interactions do not play a significant role on the stability of this system.

However, one can observe several interesting trends in Fig. 6 where $\Delta\Phi$ and μ are plotted as a function of coverage. For the on-surface adsorption $\Delta\Phi$ is negative, and for the substitutional adsorption $\Delta\Phi$ is positive. Since Co and Cu have almost the same electronegativity (1.88 and 1.90, respectively), the change of the work function is a geometric effect. In the case of on-surface adsorption the result is in line with the observations for homoepitaxial metallic systems where surface roughness leads to a reduction of the work function[25,26] as a consequence of the so-called Smoluchowsky smoothing. Analogous to findings for Na on Al(001),[27] for the on-surface adsorption $\Delta\Phi$ exhibits a nonmonotonic behavior as a function of coverage. At shorter distances, i.e., at higher coverages (e.g., above 0.5 ML), the effect of *depolarization* is responsible for the decrease of $\Delta\Phi$; namely, the repulsive electrostatic interaction is reduced by a decrease of the dipole moment.

In contrast to the on-surface adsorption where the adatom lies above the surface, for the substitutional adsorption the adatom relaxes inwards (-4%) with respect to the surface substrate layer and therefore the induced dipole moment has the opposite sign. Due to the better screening of the surrounding substrate atoms, $\Delta\Phi$ and μ show a much weaker dependence on coverage. Note that Fig. 6 assumes that the Co coverage is always homogeneously distributed. In reality in particular for the on-surface adsorption at $\Theta\geqslant 0.30$ ML we expect a phase transition towards compact Co islands. Thus the work function will abruptly change to 5.31 eV for a $p(1\times1)$-Co structure.

Finally we would like to mention, that intermixing for low coverages goes together with surface strain relief. Pseudomorphic thin films of Co on Cu(001) with a thickness of 1–2 ML are subject to tensile strain due to the lattice mismatch of the two materials.[28] In the dilute limit the incorporation of single Co atoms in the substrate layer might represent a more effective mechanism with respect to surface strain relief compared to the formation of compact on-surface islands with a reduced in-plane lattice constant.[29] As a consequence the Co adatoms are expected to be homogeneously distributed on the surface and an intermixed surface layer is likely to occur for $\Theta\leqslant 0.25$ ML.

V. INFLUENCE OF MAGNETISM ON THE ADSORPTION ENERGY

Since the ground state of cobalt is ferromagnetic, we investigate in this section the influence of magnetism on the stability of the studied systems. The adsorption energies of nonmagnetic and spin-polarized adsorbate systems as a function of coverage are plotted in Fig. 7. We see that the magnetic solutions are always more favorable than the nonmagnetic. The energy gain due to spin polarization is somewhat stronger in the case of on-surface adsorption compared to substitutional adsorption, e.g., for $\Theta=0.25$ ML, $\Delta E^{\mathrm{sp}}_{\text{on-surface}}=0.27$ eV and $\Delta E^{\mathrm{sp}}_{\mathrm{subst}}=0.20$ eV. This effect can be explained by the lower coordination of the adsorbate on the surface which results in a stronger localization of the Co $3d$ states and a larger gain in magnetic energy. However, the energy difference of the two investigated adsorption geometries—on-surface and substitutional—changes by less than 0.1 eV for a $p(2\times2)$ unit cell if spin polarization is considered: $\Delta E^{\mathrm{ad}}_{\mathrm{NM}}=1.32$ eV for a nonmagnetic calculation compared to $\Delta E^{\mathrm{ad}}_{\mathrm{sp}}=1.24$ eV for a spin-polarized calculation. We note that in this paper we are interested in adsorp-

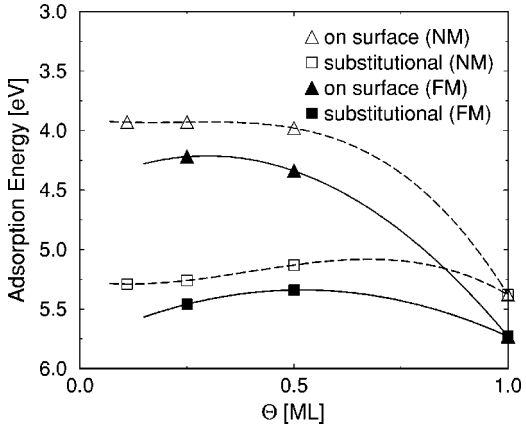

FIG. 7. The adsorption energy E^{ad} of a Co adatom on a fcc hollow (triangles up) and a substitutional (squares) site as a function of coverage for nonmagnetic (open symbols) and ferromagnetic (solid symbols) systems. In the limit of $\Theta=1.0$ ML both adsorbate geometries coincide in a Co adlayer on Cu(001).

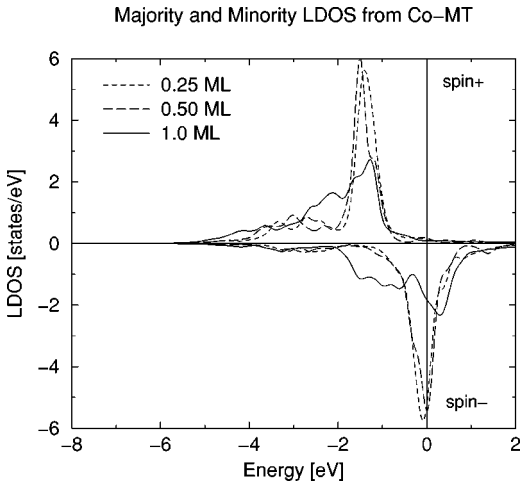

FIG. 8. *s*, *p*, and *d* contributions to the total density of states from the Co muffin tin for 0.25 ML (dotted line), 0.50 ML (dashed line), and 1.0 ML (solid line) Co adsorbed on-surface on Cu(001). Positive LDOS indicates the majority states, negative LDOS the minority states. The calculated DOS were broadened by a Gaussian with a width of $2\sigma=0.2$ eV.

tion energy *changes* and *relative* stability of different adsorbate geometries. While quantitatively the results are affected by magnetism, we find that both the magnetic and nonmagnetic descriptions give the same qualitative trends—namely, the substitutional adsorption is lower in energy than the on-surface—but with growing coverage becomes less favorable compared to the formation of compact cobalt islands.

Table I contains the magnetic moments of the cobalt adatom in the two adsorbate geometries for different coverages. For the on-surface adsorption the magnetic moment is 0.24 μ_B higher than for the substitutional geometry. This reflects the trend that a lower coordination leads to narrower *d* bands and a higher density of states at the Fermi level which according to the Stoner model enhances the tendency towards magnetism. The same effect was observed from Korringa-Kohn-Rostoker (KKR) calculations of the magnetic moments of isolated 3*d* impurities adsorbed on the Cu(001) surface or in the substrate layer.[30] The slightly higher magnetic moments in Ref. 30 compared to our study are due to structural differences: i.e., Lang *et al.* used the experimental lattice constant of copper (3.61 Å) and neglected relaxations. Our calculations show that changing the lateral parameter from the theoretical LDA value for bulk Cu (3.55 Å) to the theoretical GGA value (3.65 Å) leads to an increase of the magnetic moment of $0.2\mu_B$. The strong relaxation of the Co adatom, adsorbed at a hollow site, towards the substrate layer (-16%) goes together with a reduction of the magnetic moment.

TABLE I. Magnetic moments of cobalt in the ferromagnetic systems in (μ_B) for different coverages in the on-surface and substitutional adsorbate geometries. For $\Theta=1$ ML the magnetic moment of a $p(1\times1)$ cobalt monolayer on Cu(001) was considered.

	M (μ_B)	
Θ (ML)	On-surface	Substitutional
0.25	1.62	1.38
0.50	1.68	1.44
1.0	1.71	1.71

The magnetic moment grows slightly with increasing coverage for both adsorbate geometries which shows that at shorter distances the magnetic coupling between the Co adatoms gains importance. The increasing magnetic moment comes along with a larger exchange splitting. This is indicated in Fig. 8 by the fact that the separation between the centers of mass of the minority and majority Co bands increases with coverage.

Insight into the spacial distribution of the spin density in both adsorbate geometries is given in Fig. 9 where cross sections of the spin density along the (100) and $(1\bar{1}0)$ planes for a Co coverage of 0.25 ML are plotted. For the on-surface geometry the spin density around the Co adatom is more expanded in the vacuum region. The spin polarization induced in the substrate has a weak oscillatory character; i.e., nearest neighbors couple ferromagnetically to the Co adatom, while next-nearest neighbors couple antiferromagnetically with an absolute value of the magnetic moment in the MT sphere of approximately $0.10\mu_B$. We note that for Cu(001)-$p(2\times2)$-Co-sub the induced polarization is stronger for the nearest neighbor from the surface layer, $0.10\mu_B$, while the magnetic moment of the nearest neighbor in the subsurface layer is negligible, $0.01\mu_B$. A negative net polarization of the interstitial region of the order of $0.10\mu_B$ is found for the substitutional geometries and the $p(1\times1)$ monolayer. This polarization is due mainly to the *s* and *p* states of Cu and for 1 ML Co/Cu(001) is in line with a previous DFT result.[31] On the other hand, for the on-surface adsorption of submonolayer coverages (0.25 and 0.50 ML) the value is positive which can be attributed to the stronger expansion of the spin density of Co in the vacuum region.

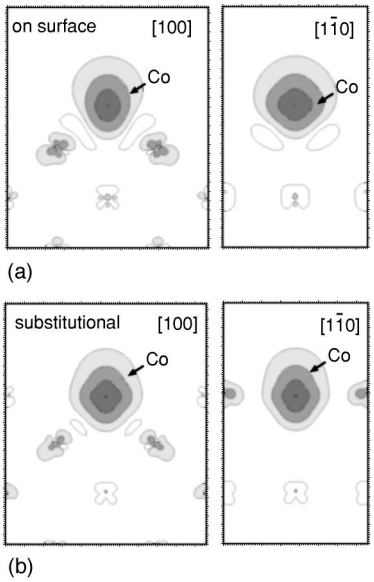

FIG. 9. Spin-density plots of a $p(2\times2)$ structure with Co adatom at on-surface (upper panel) or substitutional (lower panel) adsorption sites. The grey regions correspond to regions of positive spin density while regions of negative spin density are marked only by contour lines. The contour lines start at $\pm 10^{-3}e$/bohr^3 and have a separation of a factor of 10. The plots show a cross section along the (100) and $(1\bar{1}0)$ planes.

VI. NUCLEATION POTENTIAL OF SUBSTITUTIONAL Co ATOMS

As discussed in Sec. IV in the initial stage of growth single cobalt atoms are likely to exchange sites with copper atoms from the substrate layer. Due to the substitutional adsorption at low coverages, we have an unexpected situation on the surface: some cobalt atoms are incorporated in the substrate layer and there are cobalt as well as copper adatoms diffusing on the surface. Recently, atomic exchange was proposed as a mechanism for island nucleation and the influence of such pinning centers on island density and the island-size distributions was studied using mean-field rate equations and Monte Carlo simulations.[2,3,7] In this section we investigate quantitatively the nucleation potential of the substitutional cobalt atoms and compare to the behavior of $3d$ impurities in Fe(001).

We calculated the adsorption energy of Co and Cu atoms at hollow sites on the clean Cu(001) and the adsorbate system with $p(3\times3)$ substitutional Co atoms. The isolated adatom on the clean Cu(001)-surface is marked as ''far.'' Depending on the position with respect to the substituted Co atom there are two different adsorption sites on the Cu(001)-$p(3\times3)$-Co-sub surface: one where the adatom (Co or Cu) is the nearest neighbor [Fig. 10(a)] and another where it is $1.5a^0_{\mathrm{Cu}}$ away from the substituted Co atom [Fig. 10(b)].

In our previous work[11] the atomic positions of the substrate Cu(001)-$p(3\times3)$-Co-sub in the adsorbate systems shown in Figs. 10(a) and 10(b) were fixed to the positions of the bare substrate (as already addressed in Sec. III surface Cu atoms and substitutional Co relax 3% and 7% inwards, respectively). The height of the adsorbate above the surface was 7% and 10% shorter than the interlayer spacing in bulk copper for a Cu and Co adatom, respectively. We have now optimized the height of the adsorbate as well as of the substitutional Co. We find that the Cu adatom relaxes 10% inwards in both configurations, Figs. 10(a) and 10(b), while Co relaxes by -17% if it is $1.5a^0_{\mathrm{Cu}}$ away from the substituted Co atom [Fig. 10(b)] and by -19% as a nearest neighbor to it [Fig. 10(a)]. The height of the Co atom does not change noticeably except for the system where the Co adatom is a nearest neighbor to the incorporated Co. In this case the substitutional Co relaxes by only 3.6% inwards. Additionally the lateral relaxation for the systems in Fig. 10(a) was calculated. The most distinct feature is the contraction of the distance between the adatom and the substitutional Co, whereby the effect is much stronger in case of a Co adatom, 2.16 Å, than for Cu, 2.38 Å.

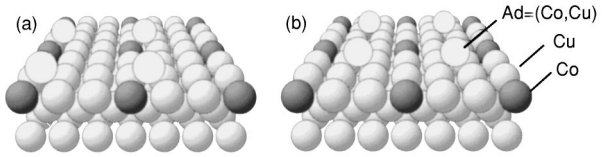

FIG. 10. Structures of (3×3) substitutional Co on Cu(001) with additional adatoms (Co or Cu) at an on-surface hollow site as (a) nearest neighbor or (b) 1.5 a^0_{Cu} away from the substituted Co atom.

The adsorption energy of these systems is calculated analogous to E^{ad} on the clean Cu(001) surface [Eq. (1)] where instead of $E^{\mathrm{Cu(001)}}$ the total energy of the Co-substituted $p(3\times3)$-Cu(001) surface is considered. The results are listed in Table. II as energy changes with respect to the ones of the isolated adatoms (''far'') on Cu(001) ($E^{\mathrm{ad}}_{\mathrm{Cu\text{-}far}}=3.68$ eV, $E^{\mathrm{ad}}_{\mathrm{Co\text{-}far}}=3.95$ eV). For all systems the structural optimization leads to a gain in adsorption energy compared to the energy of the partially relaxed geometries (energies given in brackets). The strongest effect is found for a Co adatom adsorbed as a nearest neighbor to the substitutional Co. However, the qualitative trends hold both for the partially and fully relaxed systems.

The adsorption energies show that the Co adatom is always bound stronger on the surface than the Cu adatom due to a stronger d-d and d-sp hybridization. The higher adsorption energy of Co may be considered as an implication that Co is less mobile than Cu.[33]

In order to establish the relation between energetic trends and the underlying electronic effects we have plotted the

TABLE II. Calculated adsorption energy changes of Co and Cu adatoms at a fcc hollow site on the intermixed Cu(001)-$p(3\times3)$-Co-sub surface with respect to E^{ad} for the clean Cu(001) surface. The values in parentheses correspond to the partially relaxed geometries reported in Ref. 11.

Adsorption position	$\Delta E^{\mathrm{ad}}_{\mathrm{Cu}}$ (eV)	$\Delta E^{\mathrm{ad}}_{\mathrm{Co}}$ (eV)
$1.5a^0_{\mathrm{Cu}}$	-0.03 (-0.06)	0.02 (-0.08)
Nearest neighbor	0.22 (0.16)	0.55 (0.26)

adsorption induced changes of the electron density for Cu (Fig. 11) and Co (Fig. 12) on the clean Cu(001) surface and on the Co substituted $p(3\times3)$-Cu(001) surface. Analogous to the electron density plots in Fig. 4, in the upper panels $\Delta n(\mathbf{r})$ is given with respect to the clean Cu(001) surface and a free-standing (Cu or Co) $p(3\times3)$-adsorbate layer while in the lower two panels the reference system is Cu(001)-$p(3\times3)$-Co-sub and a free-standing (Cu or Co) $p(3\times3)$-adsorbate layer. The upper panels of Figs. 12 and 4 show the on-surface adsorption of cobalt on Cu(001) for two different coverages of 0.11 ML and 0.25 ML. The adsorption induced features of $n(\mathbf{r})$ bear a strong resemblance; i.e., at distances bigger than $2a^0_{\mathrm{Cu}}$ the interaction between the adsorbates seems to be negligible. This fact is also reflected in the adsorption energies, e.g., $E^{\mathrm{ad}}_{p(3\times3)}=3.95$ eV and $E^{\mathrm{ad}}_{p(2\times2)}=3.94$ eV.

The upper two panels in Figs. 11 and 12, visualizing the electron density changes upon adsorption of a Cu or Co adatom on the clean Cu(001) surface and on the substituted $p(3\times3)$ surface $1.5a^0_{\mathrm{Cu}}$ away from the embedded Co atom, also look very similar. Indeed, the corresponding adsorption energies are close, which confirms the previous statement that the adatoms are practically not sensitive to the environment going beyond second-nearest neighbors.

A comparison of the two adsorption sites on the substituted surface in Figs. 11 and 12 makes the role of the incorporated Co atoms as *pinning centers* distinct. In the case where the adatom adsorbs as a nearest neighbor of the incorporated Co (lowest panel in both figures) the changes of electron density are much more dramatic and show a substantial asymmetry, i.e., a stronger electron charge redistribution takes place on the line connecting the adsorbate with the embedded Co. A depletion of the electron density occurs on the vacuum side of the adsorbate while $\Delta n(\mathbf{r})$ increases substantially between the adsorbate and the substituted Co atom. We note that the electronic changes are clearly stronger for the Co adatom than for the Cu adatom, and with respect to energetics, the effect of pinning is 2 times stronger for Co (0.53 eV) than for Cu (0.25 eV). The consequences of pinning on surface morphology are discussed elsewhere.[11]

In a recent DFT study applying the KKR method Nonas *et al.*[9] report a strong tendency towards substitutional adsorption also for $3d$ transition-metal adatoms on Fe(001). However, in contrast to Co on Cu(001), they found that the pair complex [Fig. 10(a)] is unstable and the Fe adatom would prefer to diffuse away from the incorporated $3d$ impurity. This is partly due to the magnetic coupling of the $3d$ impurity or Fe adatom to the magnetic substrate, partly, as in the case of a Cu impurity, it can be understood in a simple bond-cutting model: Fe-Fe bonds are stronger than Fe-Cu-bonds. Thus the system prefers to maximize the number of Fe-Fe bonds. In the case of Co on Cu(001) the situation is the opposite: Co-Co bonds are stronger than Co-Cu bonds, while the latter are stronger than Cu-Cu bonds. The effect of pinning at incorporated Co atoms is a consequence of this picture. Since this model holds also for other $3d$ elements on Cu(001) (or another noble metal substrate) the results for Co on Cu(001) should apply for a broader class of transition-

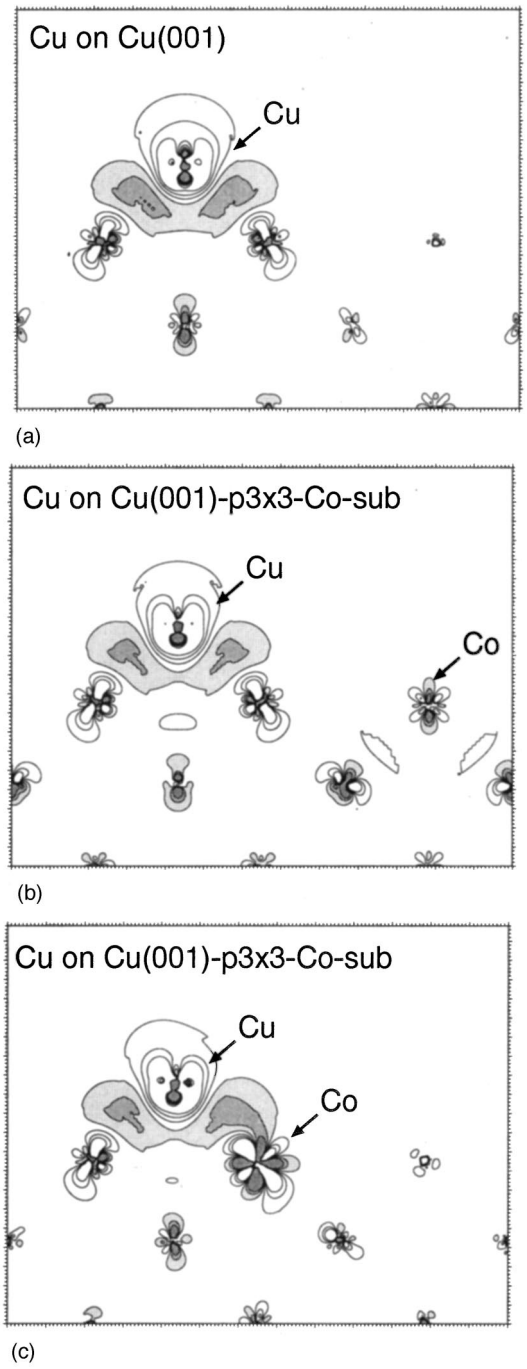

FIG. 11. Change of electron density upon adsorption of 0.11 ML of Cu on the clean Cu(001) surface (upper panel) and the system with $p(3\times3)$ substitutional Co atoms at an on-surface hollow site $1.5a^0_{\mathrm{Cu}}$ away from the substituted Co atom (middle panel) and as a nearest neighbor of it (lower panel). The adsorbate induced changes are given with respect to the clean Cu(001) surface (upper) and Cu(0001)-$p(3\times3)$-sub (lower two panels) and a free Cu-$p(3\times3)$ monolayer. The grey regions correspond to regions of electron-density increase while regions of electron-density depletion are marked only by contour lines. The contour lines start at $\pm2\times10^{-3}$ bohr^{-3} and have a separation of 4×10^{-3} bohr^{-3}. The plots show a cross section along the (100) plane.

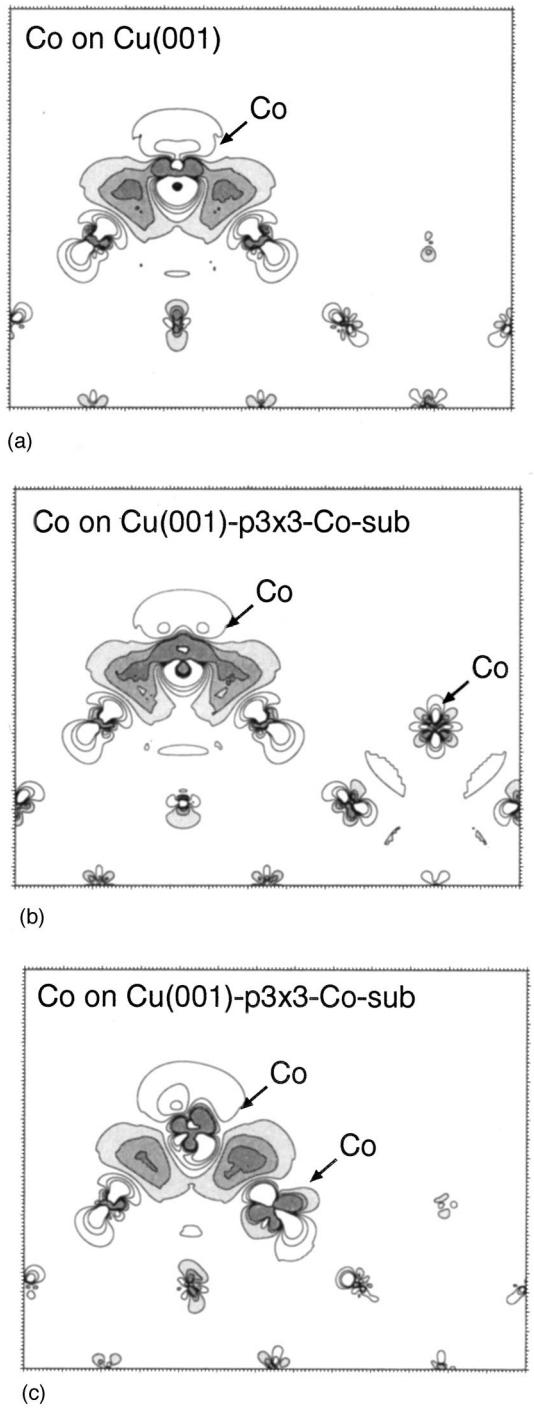

FIG. 12. Change of electron density upon adsorption of 0.11 ML of Co on the clean Cu(001) surface (upper panel) and the system with $p(3\times3)$ substitutional Co atoms at an on-surface hollow site $1.5a^0_{\mathrm{Cu}}$ away from the substituted Co atom (middle panel) and as a nearest neighbor of it (lower panel). The adsorbate induced changes are given with respect to the clean Cu(001) surface (upper) and Cu(0001)-$p(3\times3)$-sub (lower two panels) and a free Co-$p(3\times3)$ monolayer. The grey regions correspond to regions of electron-density increase while regions of electron-density depletion are marked only by contour lines. The contour lines start at $\pm2\times10^{-3}e/\mathrm{bohr}^{-3}$ and have a separation of 4×10^{-3} bohr^{-3}. The plots show a cross section along the (100) plane.

TABLE III. The adsorption energies $E^{\mathrm{ad}}_{\mathrm{LDA}}$ and $E^{\mathrm{ad}}_{\mathrm{GGA}}$ of the on-surface and substitutional adsorption geometries for different coverages calculated within the LDA and GGA, respectively, are given in eV per adsorbate atom. The lateral parameter is set to the corresponding (LDA or GGA) equilibrium lattice constant of copper.

Coverage	System	$E^{\mathrm{ad}}_{\mathrm{LDA}}$	$E^{\mathrm{ad}}_{\mathrm{GGA}}$
$\Theta=0.25$ ML	Cu(001)-$p(2\times2)$-Co	3.95	2.87
	Cu(001)-$p(2\times2)$-Co-sub	5.26	3.98
$\Theta=0.50$ ML	Cu(001)-$c(2\times2)$-Co	3.98	2.86
	Cu(001)-$c(2\times2)$-Co-sub	5.13	3.87
$\Theta=1.00$	Cu(001)-$p(1\times1)$-Co	5.38	4.08

metal elements on a noble-metal substrate. In fact similar behavior was observed recently for Fe/Cu(001),[7] Fe/Au(001),[35] and Ni/Cu(001).[36]

VII. SUMMARY

In summary, we performed DFT calculations with the FP-LAPW method for Co on Cu(001) and coverages between 0 and 1 ML. The results show that in the initial stage of growth, while still unaware of the presence of other Co adatoms, Co prefers to assume a high coordination with substrate atoms in a substitutional site as opposed to adsorption on a fourfold hollow site on the surface. However, with growing coverage the exchange processes become less likely compared to the formation of compact Co clusters. Although the magnetic solutions are always lower in energy, the energetic trends remain unaffected by magnetism. The polarization induced by the magnetic Co adatom in the substrate has an oscillatory character in both vertical and lateral directions and indicates that the magnetic coupling of the adatoms is mediated by the substrate.

A consequence of the substitutional adsorption in the initial stages of growth is that besides the embedded Co atoms there are not only Co but also Cu adatoms diffusing on the surface. The DFT calculations show that the incorporated Co atoms act as nucleation centers for Co and Cu adatoms on the surface, the effect being considerably stronger for Co adatoms. The analysis of the electronic and structural changes supports this picture.

The substitutional adsorption of Co on Cu(001) and the pinning at incorporated Co adatoms can be understood as a result of the relative strength and competition between adsorbate-adsorbate, adsorbate-substrate, and substrate-substrate bonds. This suggests a similar behavior for other transition-metal elements on a noble-metal substrate as indicated in recent experiments for Fe/Cu(001),[7] Fe/Au(001),[35] and Ni/Cu(001).[36]

ACKNOWLEDGMENTS

We gratefully acknowledge useful discussions with J. Neugebauer and C. Stampfl, and the stimulating collaboration with F. Nouvertné, U. May, U. Korte, and G.

Güntherodt. The work was supported by the DFG through SFB290.

APPENDIX

In order to investigate the importance of nonlocal exchange and correlation effects on the adsorption energies we performed calculations with the LDA (Ref. 12) and with the GGA (Ref. 13) for adsorbate systems with Co adatoms at on-surface and substitutional sites for different coverages. The lateral parameter was set to the lattice constants of copper obtained within the LDA and GGA approaches, respectively. The LDA value of 3.55 Å is 1.7% smaller than the measured one, 3.61 Å, while with the GGA the lattice parameter (3.65 Å) is 1.1% bigger than the experimental value (zero-point vibrations are neglected in the theory). The results are given in Table III.

The difference between $E^{\mathrm{ad}}_{\mathrm{LDA}}$ and $E^{\mathrm{ad}}_{\mathrm{GGA}}$ is of the order of 1 eV. This behavior is consistent with results for other adsorbate systems.[34] The main reason is that while the LDA overestimates cohesive energies, a substantial improvement can be achieved within the GGA. Especially in the description of the free Co atom needed as a reference system in Eq. (1) nonlocal exchange and correlation effects become important because the electron density gradient is large. However, E^{ad} is calculated per adsorbate atom. Thus the effects cancel partially if we look at adsorption energy differences. For example, for $\Theta=0.25$ ML the substitutional adsorbate geometry Cu(001)-$p(2\times2)$-Co-sub is favored over the on-surface Cu(001)-$p(2\times2)$-Co by 1.31 eV within the LDA and by 1.11 eV within the GGA. Thus, although the absolute values of the adsorption energy change, the qualitative trends are the same within the LDA and GGA.

[1] P. Ruggerone, C. Ratsch, and M. Scheffler, in *The Chemical Physics of Solid Surfaces*, edited by D.A. King and D.P. Woodruff (Elsevier Science, Amsterdam, 1997), Vol. 8.

[2] J.A. Meyer and R.J. Behm, Surf. Sci. **322**, L275 (1995).

[3] A. Zangwill and E. Kaxiras, Surf. Sci. **326**, L483 (1995).

[4] A. Schmalz, S. Aminpirooz, L. Becker, J. Haase, J. Neugebauer, M. Scheffler, D.R. Batchelor, D.L. Adams, and E. Bogh, Phys. Rev. Lett. **67**, 2163 (1991); C. Stampfl and M. Scheffler, Surf. Rev. Lett. **2**, 317 (1995).

[5] J. Neugebauer and M. Scheffler, Phys. Rev. B **46**, 16 067 (1992).

[6] M. Wuttig, Y. Gauthier, and S. Blügel, Phys. Rev. Lett. **70**, 3619 (1993).

[7] D.D. Chambliss and K.E. Johnson, Phys. Rev. B **50**, 5012 (1994).

[8] A. Davies, J.A. Stroscio, D.T. Pierce, and R.J. Celotta, Phys. Rev. Lett. **76**, 4175 (1996).

[9] B. Nonas, K. Wildberger, R. Zeller, and P.H. Dederichs, Phys. Rev. Lett. **80**, 4574 (1998).

[10] J. Fassbender, R. Allenspach, U. Dürig, Surf. Sci. **383**, L742 (1997).

[11] F. Nouvertné, U. May, M. Bamming, A. Rampe, U. Korte, G. Güntherodt, R. Pentcheva, and M. Scheffler, Phys. Rev. B, **60**, 14 382 (1999).

[12] J.P. Perdew and Y. Wang, Phys. Rev. B **45**, 13 244 (1992).

[13] J.P. Perdew, K. Burke, and M. Ernzerhof, Phys. Rev. Lett. **77**, 3865 (1996).

[14] P. Blaha, K. Schwarz, and J. Luitz, computer code WIEN97, A Full Potential Linearized Augmented Plane Wave Package for Calculating Crystal Properties, Karlheinz Schwarz, Technical University Wien, Vienna, 1999); updated version of P. Blaha, K. Schwarz, P. Sorantin, and S.B. Trickey, Comput. Phys. Commun. **59**, 399 (1990).

[15] M. Petersen, F. Wagner, L. Hufnagel, and M. Scheffler, Comput. Phys. Commun. **126**, 294 (2000).

[16] B. Kohler, S. Wilke, M. Scheffler, R. Kouba, and C. Ambrosch-Draxl, Comput. Phys. Commun. **94**, 31 (1996).

[17] H.J. Monkhorst and J.D. Pack, Phys. Rev. B **13**, 5188 (1976).

[18] P.H.T. Philipsen and E.J. Baerends, Phys. Rev. B **54**, 5326 (1996).

[19] The adsorption of a Cu adatom at a kink site does not alter the structure on the surface; i.e., the kink is only moved by one atom farther. Thus, adsorption of a Cu adatom at a kink site equals adding an additional bulk Cu atom to the system.

[20] G. Boisvert and L.J. Lewis, Phys. Rev. B **56**, 7643 (1997).

[21] N.A. Levanov, V.S. Stepanyuk, W. Hergert, D.I. Bazhanov, P.H. Dederichs, A. Katsnelson, and C. Massobrio, Phys. Rev. B **61**, 2230 (2000).

[22] S. Blügel, Appl. Phys. A: Mater. Sci. Process. **63**, 595 (1996).

[23] R. Pentcheva and M. Scheffler (unpublished).

[24] V.S. Stepanyuk, D.I. Bazhanov, A.N. Baranov, W. Hergert, A.A. Katsnelson, P.H. Dederichs, and J. Kirschner, Appl. Phys. A: Mater. Sci. Process. **71**, 1 (2000).

[25] J. Hölzl and F. K. Schulte, in *Springer Tracts in Modern Physics* (Springer, Berlin, 1979), Vol. 85.

[26] M. Methfessel, D. Hennig, and M. Scheffler, Phys. Rev. B **46**, 4816 (1992).

[27] M. Scheffler and C. Stampfl, in *Handbook of Surface Science*, Vol. 2: *Electronic Structure*, edited by K. Horn and M. Scheffler (Elsevier, Amsterdam, 1999); M. Scheffler and C. Stampfl, Phys. Rev. B **46**, 4816 (1992).

[28] Our calculations show that the lattice constant of a ferromagnetic fcc bulk phase of Co is 2.8% smaller than that of a fcc Cu crystal, while the lattice constant of a hypothetical nonmagnetic fcc cobalt crystal is 4.3% smaller than that of the copper crystal.

[29] J. Fassbender, U. May, B. Schirmer, R.M. Jungblut, B. Hillebrands, and G. Güntherodt, Phys. Rev. Lett. **75**, 4476 (1995).

[30] P. Lang, V.S. Stepanyuk, K. Wildberger, R. Zeller, and P.H. Dederichs, Solid State Commun. **92**, 755 (1994).

[31] R. Wu and A.J. Freeman, J. Appl. Phys. **79**, 6500 (1996).

[32] R. Pentcheva and M. Scheffler, Phys. Rev. B **61**, 2211 (2000).

[33] The assumption that diffusion barriers roughly scale with the energy of the initial state is plausible and has some justification.

However, we point out that a systematic investigation is necessary to prove this aspect.

[34] B. Hammer, L.B. Hansen, and J.K. Nørskov, Phys. Rev. B **59**, 7413 (1999).

[35] O.S. Hernán, A.L. Vásquez da Parga, J.M. Gallego, and R. Miranda, Surf. Sci. **415**, 106 (1998).

[36] J. Lindner, P. Poulopoulos, F. Wilhelm, M. Farle, and K. Baberschke, Phys. Rev. B **62**, 10 431 (2000).